CONTROL OF END ZONE CRACKING IN PRESTRESSED GIRDERS

Vidya Sagar Ronanki, PhD Candidate, The University of Alabama, Tuscaloosa, AL
David Burkhalter, Graduate student, The University of Alabama, Tuscaloosa, AL
Sriram Aaleti, Assistant Professor, The University of Alabama, Tuscaloosa, AL
Wei Song, Assistant Professor, The University of Alabama, Tuscaloosa, AL

ABSTRACT

In the past decade, with increased interest in long span girders, girder designs are including increasing number of prestressing strands. However, it causes cracking in the end-zone of narrow stemmed bulb-tees and I-girders, impacting the service life and design capacities. In a project funded by Alabama DOT, a 180 ft. long girder design was developed by modifying a standard Bulb-Tee girder and using a 10 ksi SCC mix. The new girder is 78 in. deep and consists of 66-0.6 in strands. The impact of draping angle, debonding on the end zone cracking was first evaluated using a 3D finite element model (FEA) developed in ABAQUS. Subsequently, the critical stresses were monitored during the detensioning process of four 54 ft. long full-scale girders with different end-zone details. It was found that the combination of limiting the draping angle and debonding the strands resulted in eliminating end-zone cracking. The detailed FEA model which was developed is also verified using experimental field data. The results of this experimental and analytical investigation will be presented in this paper.

Keywords: End zone cracking, Prestressed concrete girders, Bulb-tee, Finite element modelling.

INTRODUCTION

Significant traffic and congestion across urban areas and the current need to address the deteriorating infrastructure in the United States with limited resources creates a demand for highly durable bridges, especially long-span bridges. Economic and aesthetic considerations along with time constraints and environmental demands often result in the need for a longer span range, fewer girder lines and a minimum number of substructure units in the bridge system. Precast, prestressed concrete girders offer several advantages including, high quality, low life-cycle cost, and modularity. The standard I-shape and bulb-tee precast concrete girder sections designed and fabricated in lengths up to 160 ft constitute approximately one-third of the bridges built in the United States[1]. However, over the past decade, there was a natural progression towards increase in the girder sizes to meet the need for increased span lengths and girder spacing. Several state DOTs employed different methods including increasing number of prestressing strands in girder bottom bulb and deeper girders to meet this challenge. While this resulted in economical savings, issues related to end-zone cracking were seen in the fabrication of these long span prestressed girders. End-zone cracks were observed in spite of the design being in full compliance with AASHTO specifications[2]. These cracks can lead to moisture and chloride ingress, causing corrosion of the prestressing strands and mild steel reinforcement and negatively impacting the service life and performance of the girders. Further, in some cases, where these cracks are wider than allowable values set by an owner, it would result in a rejection of the girder. This will not only cause economic losses for a precast producer but also disrupt the construction schedule.

Previously, Alabama Department of Transportation (ALDOT) implemented bulb-tee girders that can span 165ft. During the fabrication process of these girders, some end-zone cracking issues have been observed. To address this issue, additional longitudinal mild-steel reinforcement was added into the end zone web regions. This prescriptive solution was able to reduce the cracking to certain level but could not completely solve the problem. In order to address this issue and to develop girder design for a 180 ft. long girder, an integrated experimental and analytical study was performed at university of Alabama (UA) with funding from Alabama DOT (ALDOT). As part of this study, a prestressed concrete girder design capable of spanning 180 ft., using readily available cross-section shapes with the Alabama precast producers was developed. This girder has a bulb-tee cross-section and is 78 in. deep with 7 in. thick web. The Girder was designed with 10 ksi concrete SCC mix. Following the design, four 54 ft. long test specimens with different end-zone details were fabricated. All the specimens were instrumented with concrete and steel strain gauges to monitor the critical strains during detensioning process. A detailed discussion on the experimental results from the field investigation and their comparison with the analytical models are presented in this paper.

PREVIOUS RESEARCH

A number of previous studies have investigated the end-zone cracking and effectiveness of different endzone details. A brief summary of some of these studies are presented in this section. Tuan et al. (2004)[3] investigated end zone cracking using six NU-I girders and six NU inverted-tee girders. In Phase-I of this study, endzone cracking immediately after prestress release in girders designed meeting AASHTO Specifications[2] was evaluated. In Phase-II,

specimens with modified end zone details were designed and evaluated. In Phase-I of the study, it was found that the strain in the reinforcing bars was highest at the member end and rapidly decreased as the distance from the girder end increased until total dissipation occurred at the approximate distance, *h* (where h is girder height). The results of Phase-II demonstrated that the new end zone reinforcement design improved the efficiency of the steel placement while reducing the quantity of steel used. Also, the Phase-II experiments confirmed that, using a large area of steel as close to the girder end as possible reduces the strain in vertical reinforcement and concrete cracking. The maximum stresses in reinforcement varied between 0.4 ksi and 25.8 ksi, with highest strains occurring at the girder end and rapidly decreasing with the distance from the girder end increased. Based on the results, it was recommended that, 50 percent of the splitting reinforcement is to be placed within *h*/8 from the girder end, while the rest is to be contained within *h*/2 from the girder end.

A study was conducted by Crispino et al. (2007)[4] for the Virginia DOT investigating the end zone cracking in Prestressed Bulb-Tee bridge girders. The study included the investigation of end zone cracking in current VDOT girders, the examination of a new strut-and-tie model-based design, and the fabrication of a PCBT-63 girder to verify the effectiveness of the model-based design. From this study, it was concluded that, the end-zone reinforcement should be designed with a working stress of 12 ksi for minimal, acceptable cracking. The girders with end zone details designed with 18 ksi experienced cracking with unacceptable lengths, not meeting the VDOT limits. Also, the study recommends that the region between the *h*/4 and 3*h*/4 should be considered in the end zone reinforcement design, as a significant tensile force was measured in this region.

In their work for the Wisconsin state DOT, Okumus et al. (2012)[5], performed a non-linear finite element analysis of the end zone regions of a Wisconsin BT-54 (54W girder) to understand the behavior during the detensioning process. The results from the finite element models were then verified using experimental data from two 54W girders. A good agreement was seen between the cracks predicted by the finite element model and measured values from the field. After establishing parity with field results further models were used to examine the effect of release sequence, the effect of increased vertical reinforcement in the end zone and the effect of debonding. Based on these finite element models it was observed that using large vertical bars at the girder end limits the strains in the web area. Debonding the strands at the girder end directly lowers the stresses transferred to the concrete and controls extent of cracking. It was also observed that changing the cutting sequence does not particularly influence endzone cracking. A similar study was also performed by Arab et al. (2014)[6], using a 205 ft long, Washington state DOT's WF100G super girder consisting a total of 80-0.6 in. strands. This investigation carried out on the full span girder reaffirmed the recommendations made by Tuan et al. (2004)[3]; i.e. 50 % of the endzone reinforcement should be placed within h/8 and the remainder should be placed between h/8 and h/2 to minimize cracking. Hamilton et al. (2012)[7] performed a multi-component test program for the Florida DOT to evaluate the effects of web splitting, flange splitting, and lateral splitting on Florida I-beam**s**. This study concluded that, partial debonding was effective in controlling the length and width of the web splitting cracks. Further, it was also seen that increasing vertical end zone reinforcement compared AASHTO requirements decreased the length and widths of the web splitting cracks.

SPECIMEN DESIGN AND FINITE ELEMENT ANALYSIS

The design and detailing of BT-78 was carried out as per the current practices of ALDOT and the requirements of current AASHTO LRFD[2] code specifications. The girder section was designed to span a distance of 180 ft, at 6 ft. girder spacing. The maximum service level and ultimate moment demand at the girder mid-span is calculated to be 10646 kip-ft and 14673 kip-ft respectively. The girder was designed to resist a maximum shear force of 398 kips under factored loading. As per ALDOT requirements the girder was designed to have zero top tensile stresses at release and zero tensile stresses under service loads. This resulted in BT-78 section made of 10 ksi concrete, with a total of 66-0.6 in. dia strands, including 22 draped strands. The cross sectional details of the BT-78 girder are shown in Fig. 1a. The cracking and nominal moment capacity of the girder are calculated to be 11694 kip-ft and 22442 kip-ft respectively. Following the AASHTO[2] requirements, the end-zone reinforcement was designed and detailed to resist 4% of the prestressing force. This resulted in #7 and #5 bars at 4 in. spacing for end-zone reinforcement. The details of the end-zone reinforcement are shown in Fig. 1b.

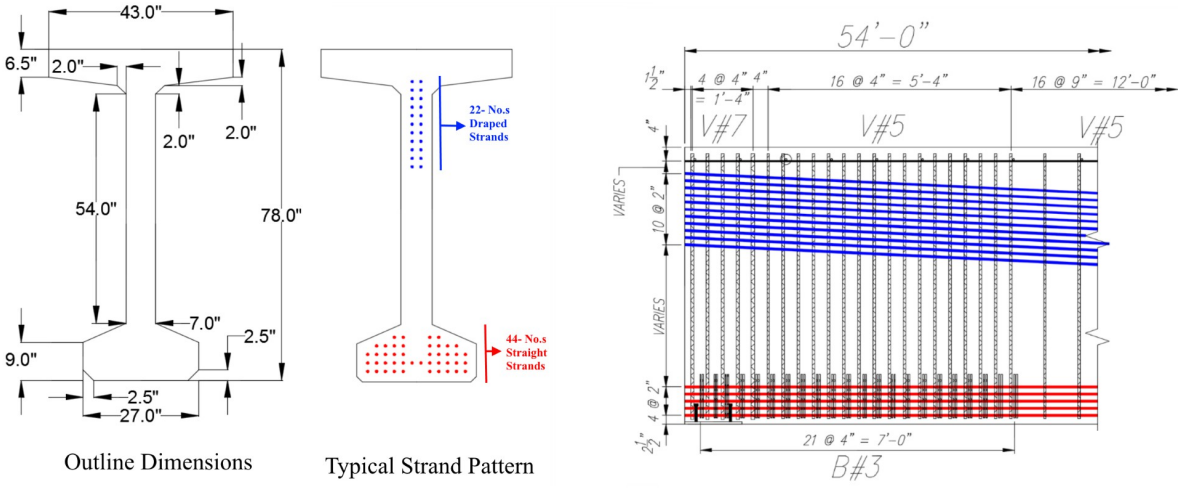

a) Cross sectional details b) Typical Endzone details

Fig. 1 Cross-section and end-zone details of standard BT-78 girder

Following the design of standard BT-78, a detailed 3D finite element analysis (FEA) model was developed in ABAQUS[8] to investigate the impact of several end-zone details on mitigating the endzone cracking. Several alternatives to the standard design including a change in the configuration of prestressing strands (lower draping and debonding), increasing the area of vertical stirrups in the end zone and introducing horizontal steel were investigated. Taking advantage of girder symmetry along its length and across the cross-section, only half the length and half the cross section of the full size girder was modelled to minimize the computational time. The quarter size girder model was divided into three zones, depending on the nature of concrete and steel stresses expected in those regions (see Fig. 2a). Zone-1 extended over a length of 60 d_b (where d_b = diameter of strand) from the girder end, where the prestress is assumed to be transferred to surrounding concrete. This region is of primary interest as cracking is typically initiated in this zone and propagated further. The concrete in this zone was modeled using concrete damaged plasticity model accounting for non-linear material behavior. A finer mesh size was used in this zone compared to the rest of

the girder. This enabled us to effectively capture the critical stresses and strains in concrete and steel reinforcement. Zone-2 was extended up to two times the height of the girder from the end and remainder of girder is designated as Zone-3. Concrete in Zone-3 was modelled using linear elastic material to minimize the computational time. The effect of the strands and the prestressing force from individual strand is applied as a surface traction force on concrete around each individual strand over a transfer length taken as 60 times the diameter of the strand as per AASHTO LRFD Bridge Design Specifications[2] 5.11.4.1 (see Fig. 2b). The end-zone reinforcement was explicitly modelled using truss elements and the behavior was modelled using linear elastic material model.

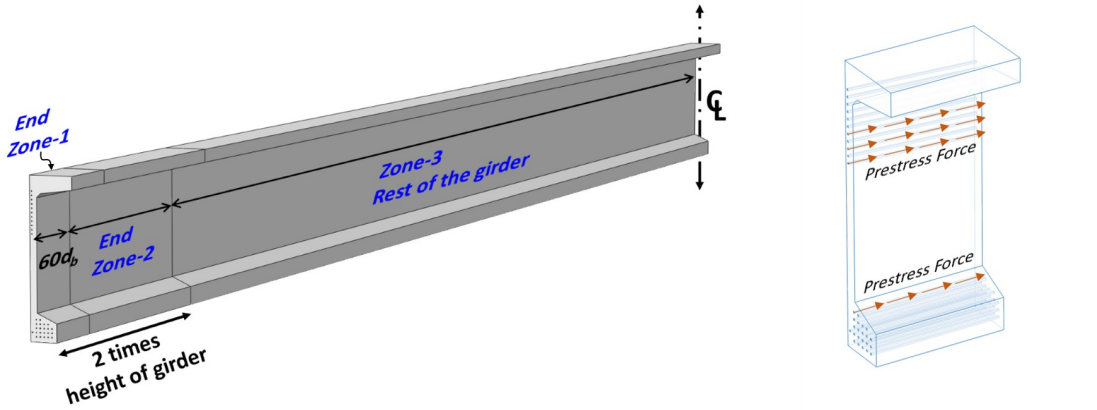

a) Abaqus model with end regions marked

b) Application of prestress force

Fig. 2 Abaqus model for BT-78 girder

Fig. 3 shows the critical stresses in the standard girder (Specimen-1) end-zone immediately after transfer of all the prestressing force. Three major areas of cracking were observed in the finite element analysis of specimen-1. These regions are designated as regions (1), (2) and (3) as shown in Fig. 3a. Crack region-(1), started just below the lowest draped strands and has the highest tensile strains with cracks expected to extend about 20 to 30 inches from the girder end. Cracks in regions (2) and (3) are expected to form around the mid height and web-to-bottom bulb intersection, with multiple cracks of limited length as shown in Fig. 3b are expected.

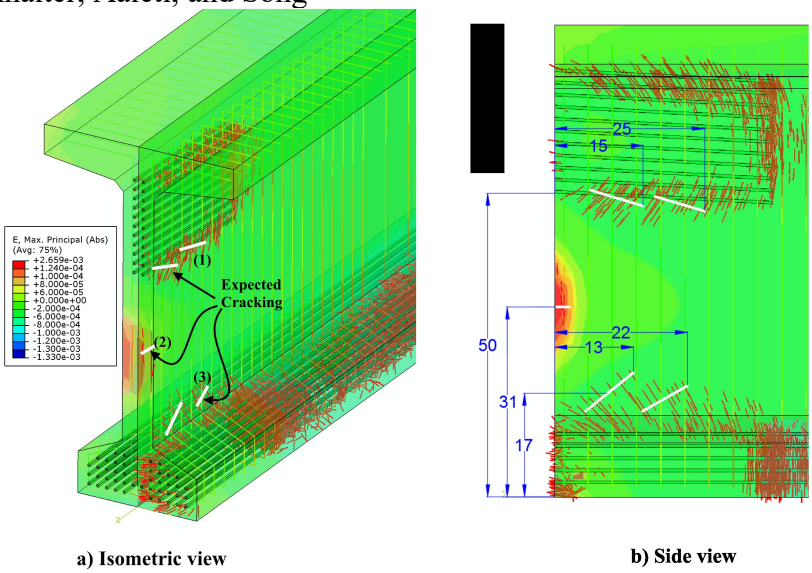

a) Isometric view b) Side view

Fig. 3 Distribution of concrete strains in endzone region of Specimen-1

The prestress transfer induces compressive strains along girder length and tensile strains along the girder depth. The FEA model shows that the presence of draped strands puts the web in a higher tensile strain state and increases the extent of cracking that would otherwise be caused just by the bottom strands. An overall reduction in the stress state of the ends would reduce the extent of inclined crack formation. This effect can be achieved by debonding the strands. Thus, a finite element model of the girder with debonded strands (Specimen-2) was developed. Further, the FEA model also indicated that the moment caused by the eccentricity between the draped strands and straight strands creates a bending effect across the girder depth leading to web cracking. This web cracking can thus be reduced by lowering the draping angle. Test Specimen-3 was developed to investigate this effect.

Finite element models of girders with increased vertical reinforcement and the presence of horizontal rebar in endzone were also investigated. It was noticed that an increase in vertical reinforcement did not affect the stress state of the end zone. There was a reduction observed in the stresses of the rebar from the standard design (7.7 ksi) to this model (6.9 ksi). It has to be noted that both these stresses are well below the AASHTO specified limit of 20 ksi and any increase of reinforcement would cause congestion problems at site. Thus this test case was deemed redundant and no test specimens were made with increased reinforcement. In the model with horizontal reinforcement, no significant effect was observed in the concrete strains. Further, the stresses in the horizontal rebar were less than 0.5 ksi indicating the ineffectiveness of these bars. Thus no test specimens were developed with horizontal reinforcement bars. The lack of utilization of these horizontal rebar is in line with the field observations made by Arab et al.[6]

Based on the FEA results, details for a total of four test specimens, including the standard design (Control, Specimen-1) were finalized. The other three test specimens had, (1) 44 straight strands with ten strands partially debonded and 22- draped strands with standard draping angle (Specimen-2); (2) 44 straight strands and 22- draped strands with lower draping angle (Specimen-3); and (3) 44 straight strands with ten strands partially debonded and 22- draped strands with lower draping angle (Specimen-4). The draped strands on

Specimen 1 and Specimen 2 had a draping angle of 2.9 degrees. Specimen 3 and 4 contained a lowered draping angle of 1.67 degrees. Sheathing was added to lower flange strands in Specimens 2 and 4 according to the debonding requirements in AASHTO LRFD Specifications[2]. A summary of draping angle and debonding criteria of the four test specimens is shown in Table 1. Fig. 4 shows the expected cracking in the selected test specimens from the finite element analysis. The red lines in Fig. 4 indicate the principal strain vectors, and the white lines indicate the possible crack formation. Fig. 5 gives the cross-sectional details of the test specimens.

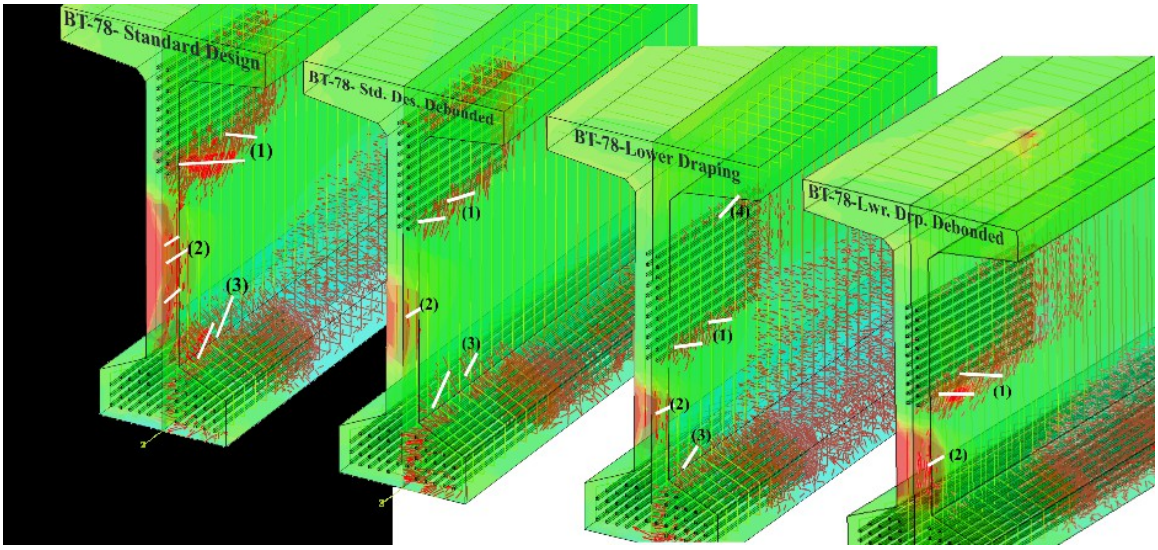

Fig. 4 Results of FE analysis showing likely regions of cracking

Table 1 Specimen configuration

	Specimen 1	Specimen 2	Specimen 3	Specimen 4
Draping Angle	2.9°	2.9°	1.67°	1.67°
Debonding	No	Yes (18%)	No	Yes (18%)

SPECIEMEN CONSTRUCTION AND INSTRUMENTATION

Four 54 ft. long BT-78 girder specimens representing the end 54 ft segment of the 180 ft. long girder were cast at the Fortera precast yard in Pelham, Alabama. The reduced length for specimens was chosen due to restrictions on the weight and length capacities for transportation and testing of the girder in the laboratory. The test girders were cast, two at a time, on the same casting bed at the precast plant. Since the test specimens were only segmented versions of the full-length specimens, and to minimize the uplift forces at draping points, the girder specimens with same draping angle were cast at the same time. Fig. 6a and 6b shows the schematic of the casting bed and the reinforcement cage respectively.

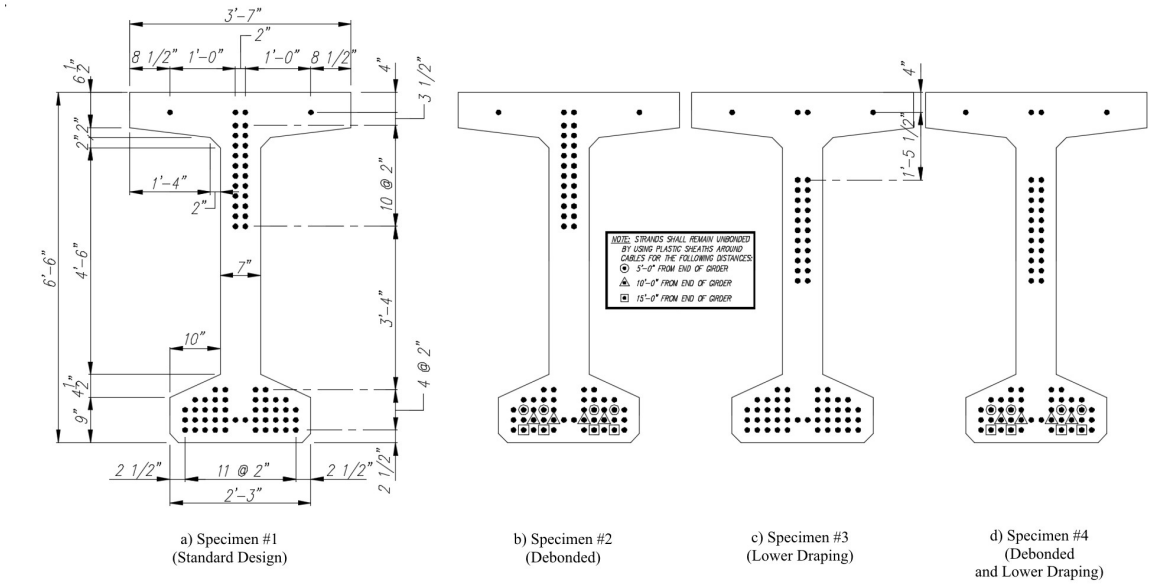

a) Specimen #1 (Standard Design)

b) Specimen #2 (Debonded)

c) Specimen #3 (Lower Draping)

d) Specimen #4 (Debonded and Lower Draping)

Fig. 5 Test specimen sectional details

All the test specimens were extensively instrumented with demountable mechanical gauge targets (DEMEC), and internal strain gauges. The DEMEC gauges were used to study the transfer length of 0.6 in. diameter prestressing strands in combination with a SCC mix. Strain gauges were used to capture the maximum tensile strains in reinforcement and concrete. While the effectiveness of each of the proposed endzone modifications can be judged by visual comparison of the extent of cracking. The data from these strain gauges would allow us quantify the endzone behavior of the four test specimens. The strain gauge locations were finalized based on the expected cracking in each specimen from the FEA models. The details of the stain gauge locations are shown in Fig.7.

FIELD OBSERVATIONS

The prestressed strands were detensioned in three phases following a predetermined cutting sequence as shown in Fig. 8. The strands were cut simultaneously at few inches outside of each of the four headers using a torch.

Cracks in endzone were observed in all the specimens except in Specimen-4 containing strands at lower draping angle and debonded strands (see Fig. 9). In general, for all the specimens, the endzone cracks grew over time, with the majority of the cracking occurring within the first 7 days after prestress release. The girder end zones were inspected for cracks for three to four times at different girder ages and crack lengths were recorded for each specimen. The summary of observed crack lengths for all the specimens is presented in Table 2. Fig. 9 shows the end-zone cracking in the all the girder specimens at one week after prestress release. The evolution of cracks in all the girders with the girder age is shown in Fig. 10.

a) Casting bed schematic

b) Reinforcement cage on casting bed

Fig. 6 Casting of test specimens at precast yard

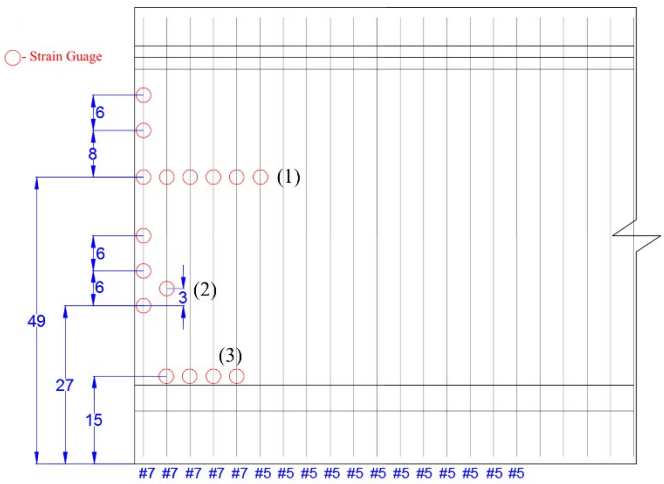

a) Strain guage locations

b) Placement of gauges in field

Fig. 7 nominal rebar strain gauge locations

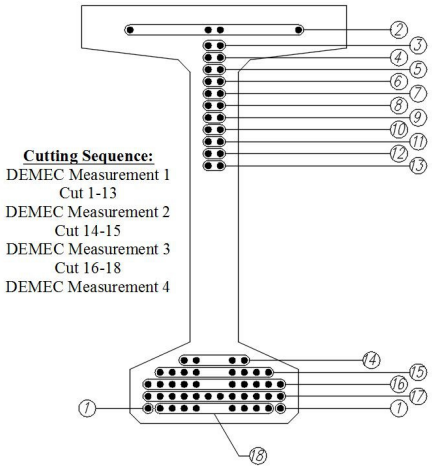

Fig. 8 Strand cutting sequence

Specimen-1, which contained fully bonded strands and strands at the standard draping angle, produced diagonal cracks in the upper portion of the web, horizontal web cracks, and cracks at both flange-web interfaces (see Fig. 9a). The diagonal cracks reached a length of 36 in extending down at approximately 35 degrees from the top of the web. The combined length cracks on both sides of Specimen-1 was approximately 300 inches. at the end of 28 days, The diagonal crack extended up to 39 inches from the girder end, or half-the height of the girder, *h*/2. Specimen- 1 contained more longitudinal web cracks and individual cracks when compared to other specimen.

Table 2 Endzone crack length growth

Specimen	Day	Cumulative Length (in.)	% Total Length
1	**0**	170	57%
	8	271	91%
	15	297	100%
	51	297	100%
2	**0**	113	61%
	8	165	88%
	15	187	100%
	96	187	100%
3	**0**	279	73%
	7	355	92%
	64	384	100%
4	**0**	0	0%
	7	26	54%
	106	49	100%

Specimen-2, which contained strands at the standard draping angle and partial debonding, produced similar crack pattern as Specimen-1 (see Figure 9B). However, compared to the Specimen-1, there were fewer and shorter cracks in Specimen-2. The longest diagonal crack was 36 in. long and propagated from the girder end at a 20 degrees angle with horizontal. There were no cracks at the bottom flange-web interface. The total crack length for the

Specimen-2 was about 185 in, a 37 percent reduction compared to the control specimen. This can be attributed the presence of debonding in Specimen-2.

Specimen-3, containing lower draping and fully bonded strands, experienced cracking in the web immediately after the release of the first strand cluster (strand rows 1-13). These were by far the longest cracks in any specimen. However, after visual inspection some of the initial cracks were believed to close after the release of the strands in the bottom flange. Both diagonal cracking and horizontal web cracking occurred in this specimen. The diagonal cracks formed after the release of the first cluster of strands were two pronged, with the vertex at 9 in. from the girder end. The longest of these diagonal cracks extended downward for 51 in. at an angle close to 45 degrees, while the upper of the two diagonal cracks traveled 20 inches at a 45 degrees above the horizontal. The combined crack lengths in Specimen-3 was 384 inches, a 30% increase compared to the control specimen. The Specimen-3 had fewer horizontal web cracks which were longer in length compared to the control specimen.

Fig. 9 Endzone cracking one week after prestress transfer and lifting

Specimen-4, which contained both lower draping and debonding, didn't experience any cracking immediately after prestress release. However, on day 7, a horizontal crack was noticed in the middle of the web on one of the girder faces, beginning 10 in. from the girder end and extending for 26 in. along the girder length at a low angle. By day 141, a similar horizontal crack was recorded on the opposite face of the girder. The longest crack extended to a distance of 35 in. from the girder end, or nearly $h/2$. The total crack length of Specimen-4 was 49 inches, an 87 percent reduction compared to the control specimen.

A more quantitative comparison of the results from the four test specimens is made by examining the strain gauge data. The maximum stresses observed in each of the instrumented reinforcing bars are presented in Table 3 below. There is a general decrease in the maximum bar stresses from specimen-1 to specimen-4. The relatively low values of stresses seen in specimen-4 are consistent with the fact that very little cracking was observed in the endzone for this girder.

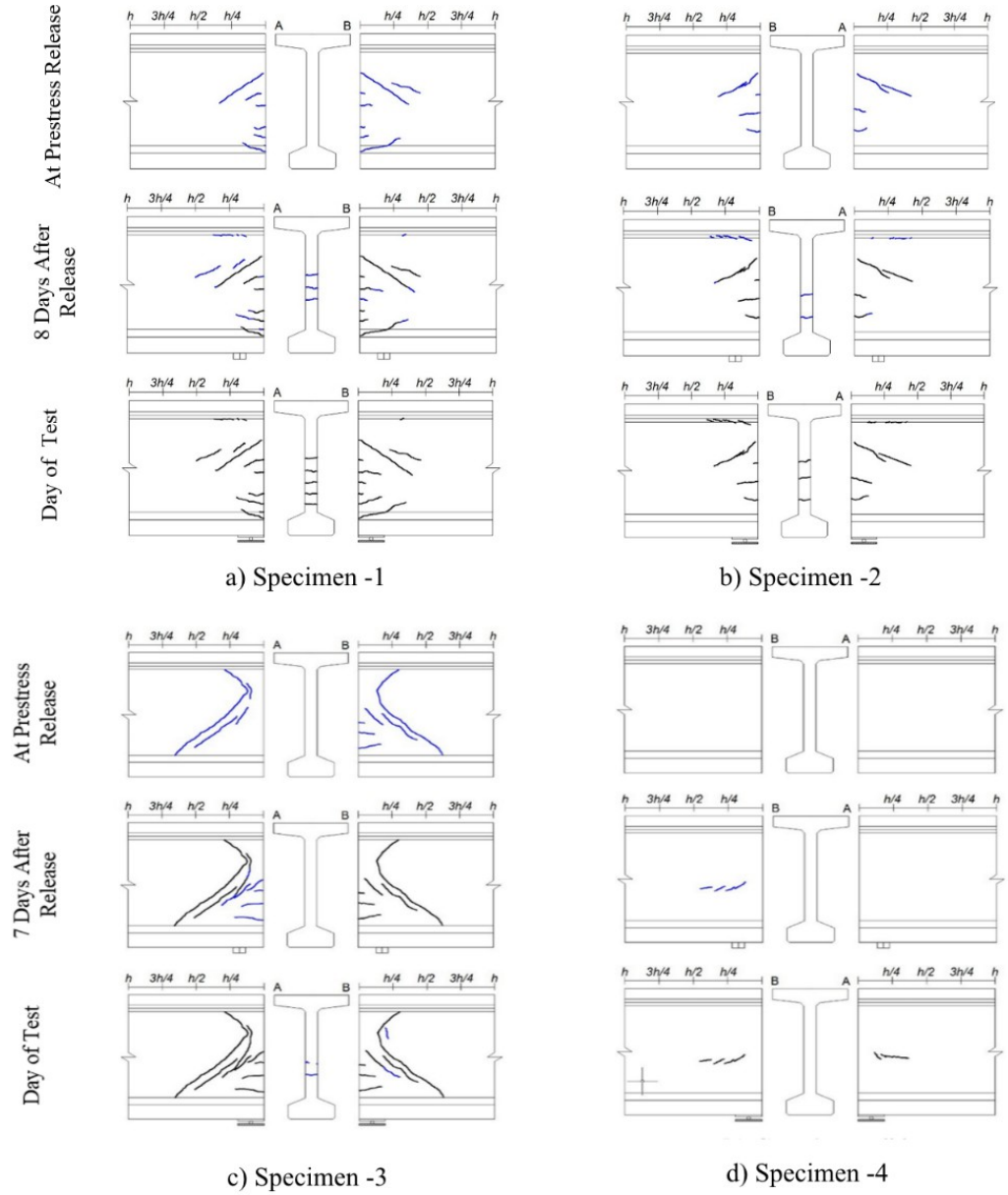

a) Specimen -1 b) Specimen -2

c) Specimen -3 d) Specimen -4

Fig. 10 Endzone cracking in test specimens

Table 3 Maximum rebar stresses

	Maximum stress (ksi)				
Specimen No.	**Bar-1**	**Bar-2**	**Bar-3**	**Bar-4**	**Bar-5**
Specimen -1	15.2	20.7	3.6	14.1	10.8
Specimen -2	11.2	5.7	5.4	5.3	15
Specimen -3	8.4	17.3	7.1	4.0	6.4
Specimen -4	1.74	4.6	-1.8	1.1	3.4

A comparison of the rebar stresses in the web cracking region of the all the specimens are shown in Fig. 11. The calculated stresses from the measured rebar strains at 39 inches and 49 inches are presented in Fig. 11a. It can be seen from this graph that the proposed solutions resulted in a reduction of end zone stresses. Fig. 11b shows the stresses across the first five vertical reinforcing bars in each of the specimens. Barring the discrepancy at bar number-3, it can be seen that the stresses in specimen-1 are generally much higher than other specimens. Fig.11 clearly shows the rebar stresses in Specimen-4 are consistently lower than those in other specimens, indicating the effectiveness of debonding with reduced draping angle in reducing endzone cracking.

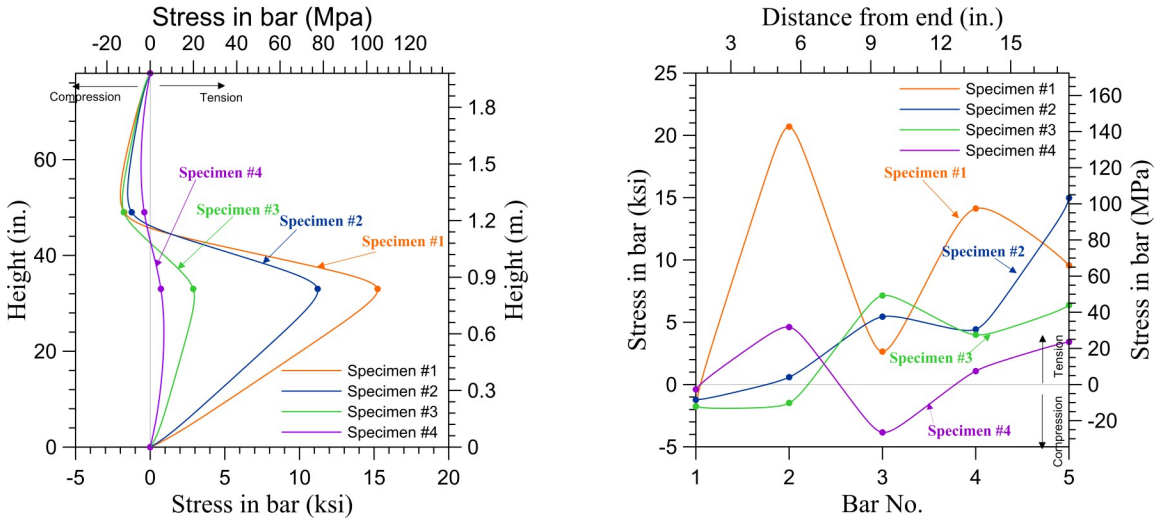

a) Web Cracking Comparision

b) Inclined Cracking Comparision

Fig. 11 Qualitative comparison of stresses in test specimen

Furthermore, the maximum vertical tensile stress values in the end zone reinforcement of all specimens measured below the AASHTO recommended design splitting force equal to 4 percent of the total prestressing force. The splitting forces were plotted against the prestressing force in Fig. 12. The total prestressing force was calculated by multiplying the 66 strands by their recorded initial prestressing force. The four strands in the top flange were not included in this calculation. The total prestressing force for the debonded specimens (Specimen-2 and Specimen-4) did not include the forces created by the twelve debonded strands. Specimen 4 produced a splitting force equal to 1.5 percent of the total prestressing force in the end zone, well below the design splitting force equal to 4 percent of the total prestressing force in the end zone.

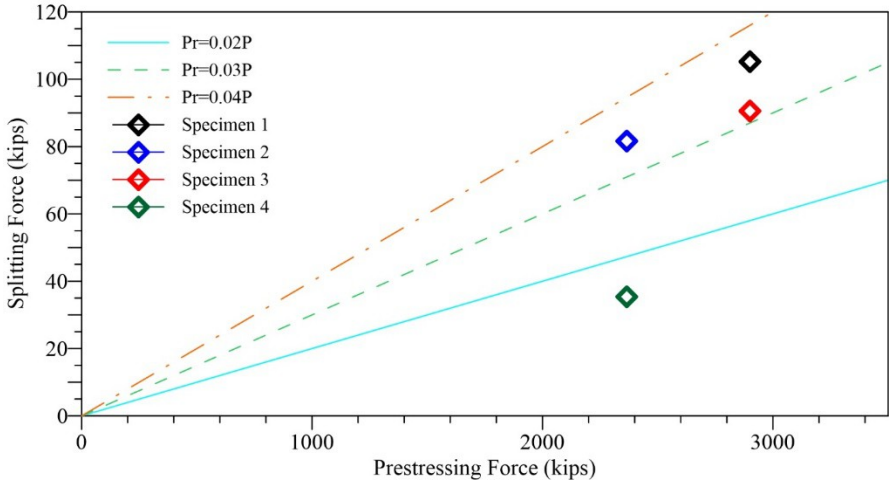

Fig. 12 Splitting force vs. Prestressing force in test specimens

TRANSFER LENGTH

Transfer length was captured immediately after a specified series of prestressing strands were cut, as well as after the final cut. The transfer lengths were found using the 95 percent average maximum strain (AMS) method[9]. The average compressive surface strain profiles of each specimen along with the average transfer lengths can be seen in Fig. 14. The dashed line represents the 95% AMS. The current AASHTO provisions were found to be conservative in estimating transfer length values.

COMPARISON WITH FE MODELS

Following the field measurements, the finite element models were updated with measured material properties at the time of casting and detensioning. A comparison of the visual cracks predicted by the finite element models with the field results are presented in Fig. 13a. It can be seen that the finite element models were accurately able to predict the location and extent of cracking. A qualitative comparison of the strain values is also shown for the inclined cracking region, for all the test specimens in Fig. 13b. The strains are plotted on the y- axis and the x-axis gives the respective rebar number or distance from the girder end. The values predicted by the finite element models closely follow the field recorded data. The results indicate that the Specimen-4, which has incorporated both debonded and lower draping strands details, was very effective in mitigating the end zone cracking. Further, the validity of the finite element models was also affirmed by comparing these models with experimental results.

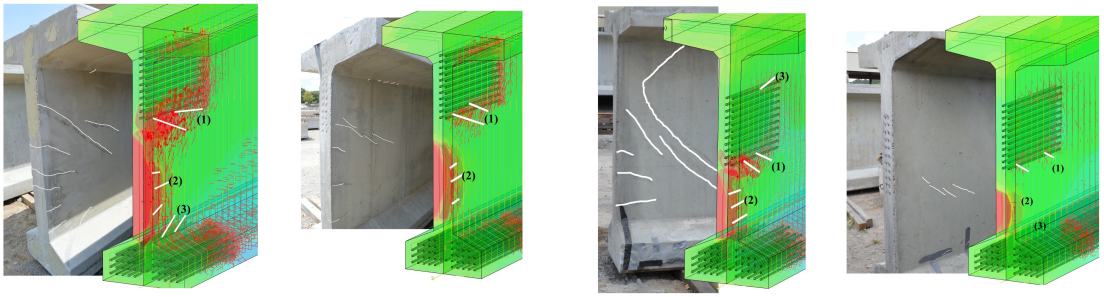

a) Comparision of visual cracks

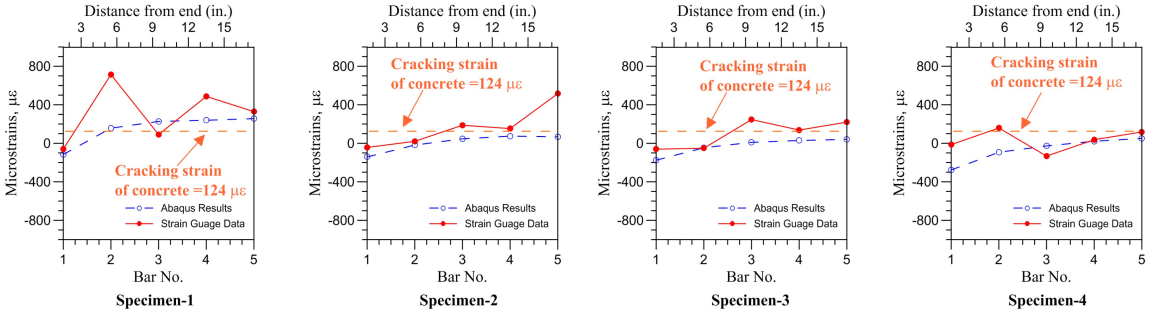

b) Comparision of strains in region (1)

Fig. 13 Comparison of cracks

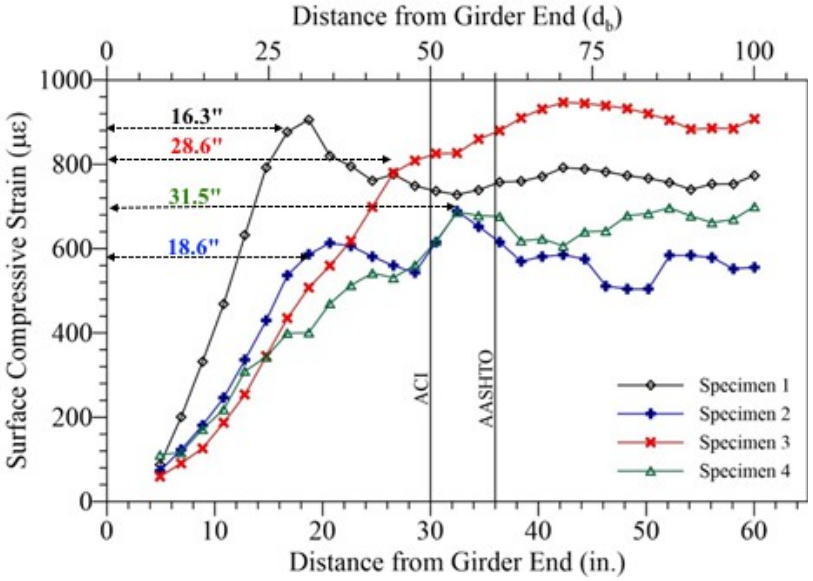

Fig. 14 Average surface strain comparison of all specimens

CONCLUSIONS

The following conclusions were reached based on the results of this study:

- Debonding twelve of the 44 strands in the lower flange reduced the total length of cracks by 53 percent from Specimen-1 to Specimen-2 and by 87 percent from Specimen-3 to Specimen-4. For the girders studied, debonding strands in the lower flange reduced the total amount of prestressing force transferred to the concrete in the end zone, resulting in a reduction in end zone cracking.

- Specimen-4, which incorporated both debonded and lower draping strands produced the least amount of cracking from prestress transfer. Lowering the draping angle in combination with debonding of strands in the bottom flange has significantly reduced the amount of cracking in the end zone by 87 percent, in comparison with the control specimen (Specimen-1).

- Cracks in the end zone grew over time in all of the cases. However, in the current project, the majority of growth occurred within the first two weeks. By day 8 after casting, 88% of the total crack length was developed in all girders, excluding Specimen-4 which showed very small amount of cracking.

- As a result of the finite element modeling, it was determined that horizontal reinforcement in the end zone webs had little-to-no effect on the reduction of principle strains in the end zone which cause splitting.

- The finite element modeling scheme developed and used in this study is in good agreement with the field results. The feasibility of any new shape or modified endzone details can be evaluated using similar modeling techniques to provide insights before implementation.

ACKNOWLEDGMENTS

The authors would like to thank Alabama DOT for sponsoring the research presented in this paper. In addition, the authors would like to acknowledge and thank Sumiden wire for donating prestressing strand needed for two test specimens. The assistance provided by Collin Sewell, Structural Lab Manager at University of Alabama along with several undergraduate and graduate students in completing the field measurements is greatly appreciated.

REFERENCES

1. Castrodale, R.W and C.D. White. *Extending Span ranges of precast Prestressed Concrete Girders,* Washington, DC: TRB, 2004
2. AASHTO. *AASHTO LRFD Bridge Design Specifications*. Washington, DC, 2014. Electronic Resource.
3. Tuan, Christopher Y., et al. "End zone reinforcement for pretensioned concrete girders." *PCI Journal* 49.3 (2004): 68-82.

4. Crispino, Eric D, Thomas E Cousins and Carin L Roberts-Wollmann. "Anchorage Zone Design for Pretensioned Precast Bulb T Bridge Girders in Virginia." 2009.
5. Okumus, Pinar, Michael G. Olivia and Scot Becker. "Nonlinear finite element modeling of cracking at ends of pretensioned bridge girders." *Engineering Structures* 40 (2012): 267-275.
6. Arab, Amir, et al. "Analytical investigation and monitoring of end-zone reinforcement of the Alaskan Way viaduct super girders." *PCI Journal* 59.2 (2014): 109-128.
7. Hamilton, H. R., Gary R. Consolazio and Brandon E. Ross. "End Region Detailing of Pretensioned Concrete Bridge Girders." 2013.
8. Dassault Systèmes Simulia Corporation. *Abaqus Analysis User's Manual (6.12)*. Providence, RI, USA: Dassault Systèmes, 2012.
9. W, Russell B and Burns N H. "Design guidelines for transfer, development and debonding of large diameter seven wire strands in pretensioned concrete girders." 1993.